Journal of Biomechanics 83 (2019) 1–8

Contents lists available at ScienceDirect

Journal of Biomechanics

journal homepage: www.elsevier.com/locate/jbiomech
www.JBiomech.com

Nano- and microscale mechanical properties of erythrocytes in hereditary spherocytosis

Maria N. Starodubtseva [a,b,*], Ekaterina F. Mitsura [c], Ivan E. Starodubtsev [d], Irina A. Chelnokova [a,b], Nikolai I. Yegorenkov [a], Lyudmila I. Volkova [e], Yuriy S. Kharin [d]

[a] Gomel State Medical University, Department of Medical and Biological Physics, Lange Str., 5, 246000 Gomel, Belarus
[b] Radiobiology Institute of NAS of Belarus, Fedyuninskogo Str., 4, 246007 Gomel, Belarus
[c] Republican Scientific and Practical Center for Radiation Medicine and Human Ecology, Ilyicha Str., 290, 246040 Gomel, Belarus
[d] Research Institute for Applied Problems of Mathematics and Informatics, Belarusian State University, Nezavisimosti Ave., 4, 220030 Minsk, Belarus
[e] Belarusian Medical Academy of Postgraduate Education, Brovki Str., 3, 220013 Minsk, Belarus

ARTICLE INFO

Article history:
Accepted 8 November 2018

Keywords:
Spherocytosis
Erythrocyte
Mechanical properties
Atomic force microscopy

ABSTRACT

Hereditary spherocytosis (HS), an erythrocyte membranopathy, is a heterogeneous disease, even at the level of the erythrocyte population. The paper aims at studying the mechanical properties (the Young's modulus, median and RMS roughness of friction force maps; fractal dimension, lacunarity and spatial distribution parameters of lateral force maps) of the cell surface layer of the erythrocytes of two different morphologies (discocytes and spherocytes) in HS using atomic force microscopy. The results of spatial-spectral and fractal analysis showed that the mechanical property maps of the HS spherocyte surface were more structurally homogeneous compared to the maps of HS discocytes. HS spherocytes also had a reduced RMS roughness and lacunarity of the mechanical property maps. The Young's modulus and averaged friction forces over the microscale HS spherocyte surface regions were approximately 20% higher than that of HS discocytes. The revealed significant difference at the nano- and microscales in the structural and mechanical properties of main (discoidal and spheroidal) morphological types of HS erythrocytes can potentially cause blood flow disturbance in the vascular system in HS.

1. Introduction

Hereditary spherocytosis (HS) is a group of inherited anemias that are characterized by the presence of significant amount of spherocytes in the peripheral blood (Perrotta et. al., 2008). HS affects 1 in 2000–5000 people of Northern European ancestry.

Mature human erythrocytes are biconcave discs (discocytes) that lack nucleus and most cell organelles. The erythrocyte shape depends on many factors including environmental factors of different nature and genetically induced molecular defects of erythrocyte structure. The diversity of non-genetically induced changes in erythrocyte shape ranges from discocyte to spherocyte, through stomatocyte and echinocyte as intermediate forms (Deuticke, 2003). Erythrocytes of four basic shape derivatives have distinct biomechanical properties (Ghosh et. al., 2016) that can be determined by various biophysical techniques, including atomic force microscopy (AFM). AFM allows probing the mechanical properties of the submicron surface layer of cells that consists of the glycocalyx, lipid bilayer and cytoplasmic layer with the cortical cytoskeleton. The thickness of this layered composite is about 30–120 nm (Deuticke, 2003; Nans et. al., 2011). The cortical cytoskeleton (membrane skeleton in erythrocytes) makes the main contribution to the mechanical parameters of this composite material. The structure of the cell surface layer can be characterized by a number of AFM parameters: the roughness, fractal dimension, parameters of Fourier transform-based methods and others (Sokolov et al., 2017; Kozlova et al., 2013; Talu et al., 2016). With AFM technique, the difference in the surface RMS (root-mean-square) roughness (R_q) was revealed for the major morphological forms of human erythrocytes (Girasole et. al., 2007; Ghosh et. al., 2016).

HS is classified as membranopathy. HS is caused by a local weakening of the contacts between the cytoskeleton and the lipid bilayer due to the mutations in genes coding proteins such as spectrin, ankyrin, protein 4.2, anion exchanger 1 (Margetis et. al., 2007; Perrotta et. al., 2008). These mutations lead to anomalies in the spatial structure of the cell surface layer and changes in the parameters of mechanical properties of the cell membrane. Transformation of discocytes into spherocytes in HS goes via vesiculation and loss of the parts of the cell membrane and cytoskeleton

* Corresponding author.
E-mail address: marysta@mail.ru (M.N. Starodubtseva).

https://doi.org/10.1016/j.jbiomech.2018.11.017
0021-9290/

(Alaarg et. al., 2013), which also changes the spatial structure of the cell surface layer. The difference in the parameters of the mechanical properties of the cell surface layer for the different morphological types of erythrocytes can specify the mechanisms of the disease genesis and development of disease complications.

Our paper aims at AFM studying the nano- and microscale parameters of the mechanical properties of the cell surface layer of discocytes and spherocytes in HS.

2. Materials and methods

2.1. Patients and blood samples

Six HS patients (average age of 10 (8; 11) years) of the Republican Scientific and Practical Center for Radiation Medicine and Human Ecology (Gomel, Belarus) were enrolled in the study. HS patients were classified as mild (1 male), moderate (2 males and 1 female), and severe (2 males). One patient (male) with clinically severe HS underwent splenectomy (9 months before the present study). All the HS patients are of Caucasian race. The study was approved by the Ethic Committee of the Gomel State Medical University. Blood test parameters for HS patients are represented in Table 1.

Human blood samples were obtained by venepuncture with patient permission under ethical consent, and anticoagulated with EDTA-K2. Thin slides were cleaned and stored in 70% ethanol before specimen preparation. Some drops of glutaraldehyde fixed (1%, 15 min) erythrocyte suspension were placed on the slides (cell monolayer) and dried at room temperature.

The analysis of erythrocyte morphology was conducted by light microscopy with microscope Nikon Eclipse E 200 (Nikon Corp., Japan) and AFM.

2.2. Atomic force microscopy

AFM was performed with atomic force microscope "NT-206" (Microtestmachines Co., Belarus) in the air at room temperature. Topographic images and lateral force maps were recorded using CSC38 type AFM probes (level B, k = 0.03 N/m, MikroMasch, Bulgaria) with scanning rate of 0.6–0.7 Hz. Lateral forces were assessed by measuring the cantilever's torsion value and represented in arbitrary units (maximal deviation of laser beam for the AFM probe torsion detected with the 16-bit analog-to-digital converter of the measuring system was 65,535 arb. units). Using lateral force maps, the following parameters of mechanical properties were calculated: median sliding friction force (F_f) and RMS roughness (R_q) of friction force maps. F_f was quantified as half of the difference of mean lateral forces sensed while scanning in two opposite directions over the area of 2.5 μm × 2.5 μm (forward and backward scans) (Starodubtseva et. al., 2012). R_q of friction force map was computed according to the algorithm of the statistical parameter estimation for indirect measurements using the values of R_q of two lateral force maps recorded in opposite directions over the area of 2.5 μm × 2.5 μm. The elastic modulus (Young's modulus, E) was assessed by force spectroscopy (force-curve analysis) using NSC11 type AFM probes (level A, k = 3.0 N/m, MikroMasch, Bulgaria) at the indentation depth of 10 nm. The force-curve analysis was performed by recording of the force value and vertical deflection of the cantilever when the AFM probe tip indents into and retracts from a cell surface at the certain point. E was calculated using the experimentally obtained force curves and Hertz model that describes the elastic deformation of the two bodies in contact under load (Starodubseva et al., 2010).

2.3. AFM data analysis

2.3.1. Spectral analysis

The AFM image with the size of $N \times N$ points was considered as a collection of N two-dimensional arrays (x, z) with N points in each for fixed values of $y \in \{1, 2, \cdots N\}$ (N is an even number); assumed here $x \in \{1, 2, \cdots N\}$, z is the values obtained after the conversion of the lateral force map into txt-file. The discrete Fourier transform was applied for each two-dimensional array (x, z) considered as a realization of a random process:

$$F(\omega_k) = \sum_{n=0}^{N-1} \left(z_n - \bar{z}\right) e^{-j\frac{2\pi kn}{N}}, k = 0, \cdots N-1,$$

where $\bar{z} = \frac{1}{N}\sum_{n=1}^{N} z_n$ is the sample mean of z, $\omega_k = 2\pi\frac{k}{L}$ is the k-th frequency, L is the length of the analyzed interval of axis x.

Using the sample spectra $F(\omega_k)$, the periodograms $R(\omega_k) = |F(\omega_k)|^2$ were plotted. For further analysis, the set $\{R(\omega_k) : k = 0, \cdots, \frac{N}{2}\}$ was only used. To obtain the statistical estimate $R_m(\omega_k)$ of the spectral density, periodogram $R(\omega_k)$ was smoothed using the Daniel window of size m. Set of N curves $\{R_m(\omega_k) : k = 0, \cdots, \frac{N}{2}\}$ is a map describing the change in the spectral estimates of the AFM image along the axis y. To get robust statistical inferences (Kharin, 2013) for AFM data the sample median of the spectral densities was calculated for each frequency ω_k:

$$\widetilde{R_m}(\omega_k) = Med\left\{R_m^1(\omega_k), \cdots, R_m^N(\omega_k)\right\}, k = 0, \cdots, \frac{N}{2}.$$

The sample median $\widetilde{R_m}(\omega_k)$ of spectral densities was approximated by two or three Gaussian functions using OriginPro® 8.0 software.

2.3.2. Fractal analysis

Fractal dimension (D_F) was calculated for lateral force maps of the cell surface (2.5 μm × 2.5 μm) using the box counting algorithm. In the modified box counting algorithm, the digital image (resolution is 256 × 256 pixels) was initially divided into 4 equal square fragments. After the calculation of D_F for each fragment, the D_F of the whole image was estimated and represented as the mean value and limits of 95% CI (confidence interval). To analyze dependence D_F on the Z-scale factor, X- and Y-data of the digital image were not changed but Z-data was multiplied by factor t that was varied in a broad range (10^{-4}–10^{6}). D_F was calculated using the box counting algorithm for each t value and the dependence $D_F = f(t)$ was plotted and analyzed (Starodubtseva et al., 2017a;

Table 1
Parameters of blood test of the HS patients.

Sample	Severity	RBC, 10^{12} cells/l	HGB, g/l	HCT, %	MCV, fl	MCH, pg	MCHC, g/l	RDW, %	Bilirubin, μM	Rt ‰
Sample 1	Mild	4.1	116	32.4	78.9	28.3	359	16.0	20–32	86
Sample 2	Moderate	3.4	109	29.0	84.5	31.7	375	17.5	27–45	264
Sample 3	Moderate	3.95	116	39.3	101.0	29.3	322	12.3	27–43	176
Sample 4	Moderate	4.29	103	28.8	67.1	23.9	356	22.7	31–99	72
Sample 5	Severe	4.19	113	31.3	74.7	28.1	376	21.9	50–91	193
Sample 6	Severe, splenectomized	5.4	149 (75*)	39.4	72.5	27.5	379	13.4	16 (55–79*)	29 (180*)

* Parameters of the blood test taken before splenectomy

Starodubtseva et al., 2017b). Fig. 1 represents averaged curves $D_F = f(t)$ for the lateral force maps of two spheroidal erythrocytes: discospherocytes (n = 33) and spherocytes (n = 43). The curves have two maxima D_{F1} and D_{F2}. The parameter of lacunarity (λ) was estimated as the squared ratio of the standard deviation to the mean for the lateral forces over the maps of 2.5 μm × 2.5 μm size (Smith et. al., 1996). Fractal properties of the lateral force maps are represented as points in space (D_{F1}, D_{F2}, λ).

2.3.3. Statistical analysis

The goodness of fit for the experimental data to normal distribution was checked with the Shapiro-Wilk's W test. Results are presented either the mean and limits of 95% CI or the median and interquartile range (Me (LQ; UQ)). The sample parameters were compared using either Student's t test or Mann-Whitney U test for normally and non-normally distributed variables, correspondingly.

3. Results

3.1. Morphology of erythrocytes in hereditary spherocytosis

Light microscopy of the HS blood smears has revealed about 60% of abnormal erythrocytes. The percentage (Me (LQ; UQ)) of discocytes, spherocytes, echinocytes, and stomatocytes (main shapes) was 39% (26%; 48%), 35% (26%; 49%), 14% (10%; 18%), and 4% (3%; 6%), correspondingly. 3D topographic images and profiles of typical discocyte, spherocytes, echinocytes, and stomatocyte in HS blood are represented in Fig. 2(a–l). Averaged diameters of prevailed morphological types of erythrocytes in HS blood (discocytes and spherocytes) were 6.25 ± 0.16 μm and 5.88 ± 0.16 μm, correspondingly (95% CI, n = 20).

The surface of some HS erythrocytes was locally granular (Fig. 2, m) with averaged granule diameter of 258 ± 32 nm (n = 50). The examples of the profile of a single granule on the erythrocyte surface, topographic image and lateral force map of the region of the erythrocyte surface with a single granule are represented in Fig. 2 (n, o). It is possible that the observed granules are extracellular vesicles (microvesicles) formed under the action of mechanical forces appeared during the preparation process. It is known that erythrocytes are one of the major vesicle-secreting cells in the circulating blood (Xiong et. al., 2012). HS erythrocytes exhibit increased vesiculation compared to normal erythrocytes (Alaarg et. al., 2013; Mullier et. al., 2012). The size of HS erythrocyte-derived microvesicles is 90–500 nm (Li et. al., 2017).

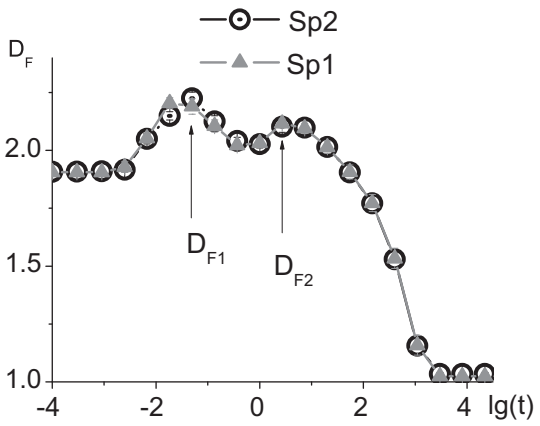

Fig. 1. Dependence of the fractal dimension on Z-scale factor for the lateral force maps of erythrocyte surface. The curves of dependences $D_F = f(t)$ for two spheroidal types (spherocyte, Sp2, and discospherocyte, Sp1) lie very close to each other. D_{F1} and D_{F2} are two main maxima of dependence $D_F = f(t)$. Data are represented as the mean and limits of 95% CI.

3.2. Spectral parameters of erythrocyte mechanical property maps in hereditary spherocytosis

The averaged sample medians of spectral estimates (Fig. 3) for the lateral force maps for discocytes and spherocytes of patients with HS differ in parameters (Table 2). The half-power bandwidth in the periodograms for discocytes is wider than that for spherocytes (Fig. 3, Table 2). The variation of the spatial period corresponding to the half-power bandwidth for discocytes is bigger in 1.19 times compared to that for spherocytes though the median for entire spectral range for discocyte is smaller than that for spherocytes (Table 2). Using the approximation of the obtained periodograms with Gaussian functions we revealed that, with comparable accuracy, the periodogram for discocytes is best approximated by three Gaussian functions and the periodogram for spherocytes by only two (Fig. 3, Table 2).

Gaussian peaks obtained for the periodograms are related to main types (subpopulations) of periodical structures in the spatial distribution of the mechanical properties of the erythrocyte surface layer. While scanning the erythrocyte surface, AFM probe "senses" the membrane skeleton (actin-spectrin network). In the actin-spectrin network in a fully stretched state, spectrin molecule has the length of about 190 nm (Liu et. al., 1987; Lux, 2016). However, the spectrin filaments of native, unstretched skeletons are much more compact with the average counter length of a spectrin tetramer of 60–70 nm and even less (Lux, 2016; Nans et. al., 2011). Obtained in our analysis the spatial periods for the periodograms characterize the average distances between junction points of the membrane and cytoskeleton. Fig. 4(a, b) show the lateral force map and topographic image of the same region of HS discocyte surface. The typical structures corresponding to three subpopulations of structural elements are concluded in circles (Fig. 4, a). Circles 1–3 show the small, middle and large structural elements corresponding to three Gaussian subpopulations of the spatial periods in Table 2. Fig. 4(c, d) represent the lateral force map and topographic image of a typical HS spherocyte. Observed simplification (increasing homogeneity) of the structure of the mechanical property maps in transition from discocyte to spherocyte are evidence of the specific way of spherocyte formation in HS via vesiculation and loss of the part of the weakened cytoskeleton with gaps in the network.

3.3. Fractal parameters of erythrocyte mechanical property maps in hereditary spherocytosis

The relief complexity of any surface can be characterized by D_F. We used D_F to study the complexity of the maps of the mechanical properties (lateral force maps) of the cell surface layer. Because the lateral force map is a physico-mathematical surface (a map of force values), there is the problem of the difference in units of measure for magnitudes presented on axis Z (units of force) and axes X and Y (units of length). Recently we have suggested using a dependence of D_F on Z-scale factor t ($D_F = f(t)$) for analysis of the fractal properties of AFM images (Starodubtseva et al., 2017a; Starodubtseva et al., 2017b). Generally, curve $D_F = f(t)$ has at least two main maxima (D_{F1}, D_{F2}). The position and height of the maxima are determined by scanning step, scanning area size and the structural features of the AFM images.

We characterized the fractal properties of HS erythrocytes by three parameters: D_{F1}, D_{F2} and λ (Fig. 5). Using such illustrative way, it can be noted that the fractal properties of the two erythrocyte morphological types are different. Herewith, parameter D_{F1} for

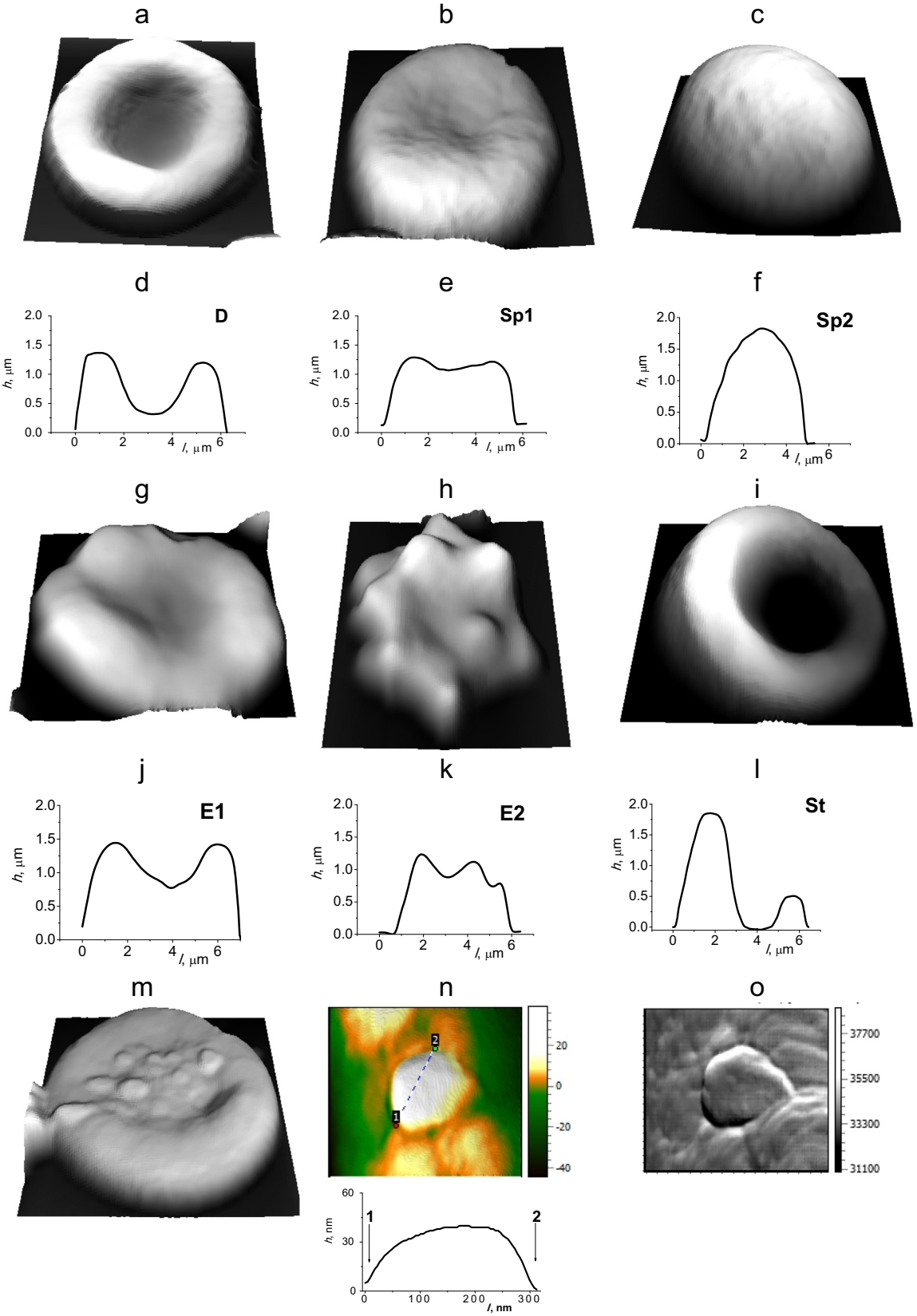

Fig. 2. AFM images of the different morphological types of erythrocytes in HS blood. (a–l) 3D Topographic images and profiles of typical cells: (a, d) discocyte (D), 6.7 μm × 7.2 μm; (b, e) discospherocyte (Sp1), 6.3 μm × 6.1 μm; (c, f) spherocyte (Sp2), 5.3 μm × 5.4 μm; (g, j) discoechinocyte (E1), 6.3 μm × 6.1 μm; (h, k) echinocyte (E2), 6.7 μm × 8.2 μm; (i, l) stomatocyte (St), 6.5 μm × 7.3 μm. (m) Discocyte with the granules on its surface, 10.4 μm × 10,4 μm. (n, o) Typical granule on the HS erythrocyte surface: (n) topographic image of the surface area, 990 nm × 880 nm, and profile between marks 1 and 2; (o) lateral force map of the same erythrocyte surface area. The resolution of images is 128 × 128 pixels.

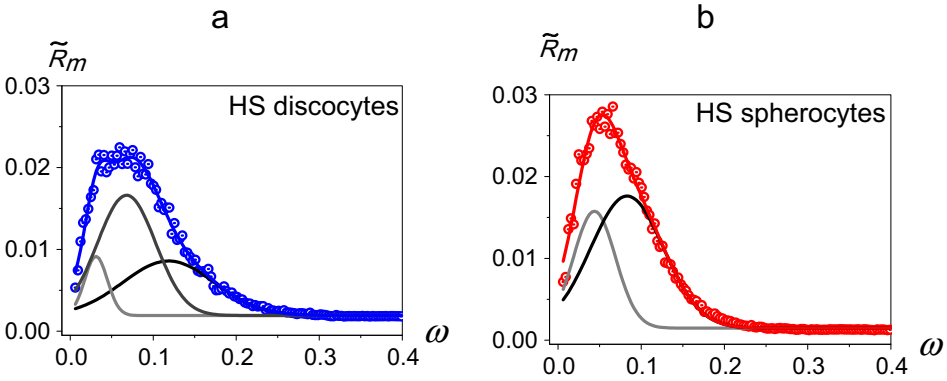

Fig. 3. Spectral estimates ($\widetilde{R_m}$) for lateral force maps of HS discocytes (a) and HS spherocytes (b). Spectral estimates for different morphological types of erythrocytes were plotted using sample medians (open circles). Spectral estimates were approximated to sums of three (a) or two (b) Gaussian functions. Gaussian function curves are colored in gray, dark gray, black (a) or on gray and black (b). Summing curves is colored in blue (a) or red (b). (For interpretation of the references to colour in this figure legend, the reader is referred to the web version of this article.)

Table 2
Spectral parameters of lateral force maps of erythrocyte surface.

Cells	Half-power bandwidth, nm^{-1}	Half-power limits for spatial periods, nm	Median value of spatial period, nm	Gaussian maxima positions and their fractions	R^2
HS discocytes	0.01007–0.12076	52–624	88	53 nm (37%), 92 nm (53%), 201 nm (10%)	99,3
HS spherocytes	0.01154–0.09723	65–544	102	76 nm (66%), 143 nm (34%)	99,2

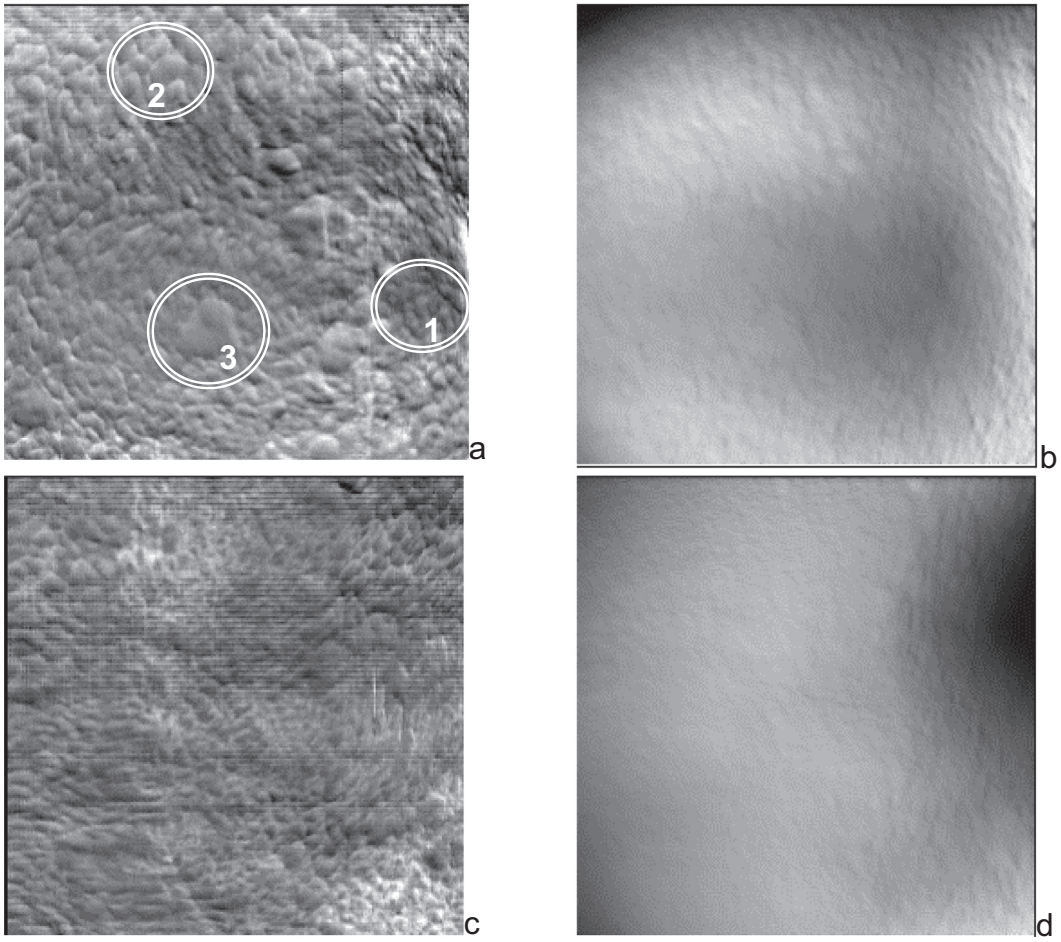

Fig. 4. Typical lateral force maps (a, c) and topographic images (b, d) of the surface of discoidal (microcytes) (a, b) and spheroidal (c, d) HS erythrocytes. In Figure a, circuits 1, 2, and 3 present the example areas with the structural elements with sizes of about 50, 90 and 200 nm, correspondingly. The plane leveling was applied to topographic images. All the represented images were processed by Gaussian and Median filters. The sizes of images is 1.5 μm × 1.5 μm, 256 × 256 pixels.

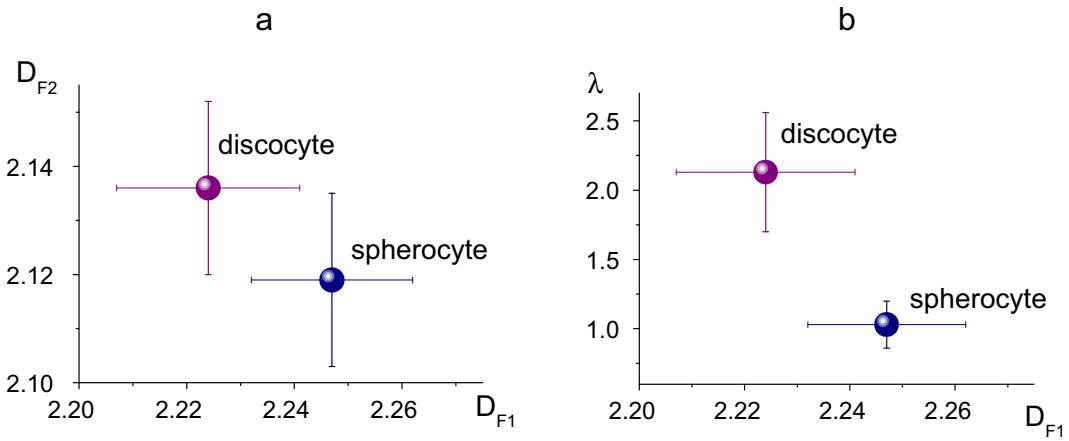

Fig. 5. Fractal parameters of the microscale lateral force maps for the erythrocytes of different morphology. D_{F1} and D_{F2} are the maxima of the curve $D_F = f(t)$, λ is lacunarity. Data are represented as the mean and limits of 95% CI.

spherocytes is significantly higher ($p < 0.05$) compared to the one for discocytes (Fig. 5, a).

Lacunarity is the measure of gappiness of fractal objects (their spatial heterogeneity). Where patterns have more or larger gaps, lacunarity is higher. Fig. 5 (b) shows that the lacunarity of the lateral force maps for discocytes is much greater than the lacunarity for spherocytes. This fact becomes clear after taking into account the results of spectral analysis of the maps discussed above. In the transformation of discocytes into spherocytes in HS blood via loss of the membrane in the most weakened sites of the cytoskeletal structure (the gaps) the structure of mechanical property maps (the membrane skeleton) changes from less homogeneous (high lacunarity) to more homogeneous (low lacunarity).

3.4. Friction and elastic properties of erythrocyte surface in hereditary spherocytosis

Spectral and fractal analysis have revealed the difference in nano- and microscale spatial distribution of the mechanical properties of the cell surface of two studied morphological types of HS erythrocytes. The specificity of the mechanical property distribution on the cell surface at the nanoscale leads to the distinction of the microscale integral mechanical parameters for the studied cell types. Table 3 represents the statistical parameters of friction forces between the AFM probe tip and cell surface during scanning process. The averaged friction forces for spherocytes were bigger than that for discocytes. The RMS roughness of the friction maps for discocytes was bigger than one for spherocytes. These findings agree to the literature data about the decrease in the RMS roughness of spherocyte surface (topographic image) compared to one of discocyte surface (Ghosh et. al., 2016).

When indenting the layered composite material with network structure like the cell surface layer, the relatively large region of the surface can be involved. The elastic modulus obtained by indenting the cell surface is not strictly "local" and characterizes the whole microscale surface region. Young's moduli of discocytes and spherocytes of HS patients are represented in Table 4. Our data show that HS spherocytes are stiffer than HS discocytes. Literature data also indicate that HS erythrocytes have a higher Young's modulus compared to the one of healthy erythrocytes (Dulińska et. al., 2006). Supposedly, in the mentioned paper, all the HS erythrocytes were spherocytes and all the healthy erythrocytes were discocytes. In our experiments, the tendency of the increase of elastic modulus in sequence "HS discocyte - HS spherocyte" also coincides with the observed tendency for the parameters of the frictional properties of the corresponding morphological forms. Meanwhile, all the parameters mentioned above characterize the mechanical property of the microscale regions of the cell surface. In general, spherocytes of HS patients are stiffer, less deformable, more elastic and frictionally resistive compared to HS discocytes.

4. Discussion

HS is a heterogeneous disease in all aspects: clinically, biochemically, and genetically (Eber and Lux, 2004). Our findings show that HS is the heterogeneous disease in mechanical properties at the level of erythrocyte population in blood even at the nano- and microscales. In the HS erythrocyte population there is a high percentage of cells of the specific morphology with the distinct mechanical properties. Using AFM, we have studied the structural and mechanical properties of two basic morphological types of HS erythrocytes: discocytes and spherocytes. These morphological types are among the types proper to the erythrocytes of healthy people. Some hypothesizes were put forward to explain the morphology transformation ("discocytes - spherocytes") of normal erythrocytes under different conditions (Lim et. al., 2002; Deuticke, 2003). The abnormal morphological transformation taken place

Table 3
Friction parameters of the erythrocyte surface.

Cell type	$F_f/F_{f\text{-}D}$, rel. units	$R_q/R_{q\text{-}D}$, rel. units	n
Discocyte	1.00 (0.80;1.33)	1.00 (0.70; 1.35)	45
Spherocyte	1.19 (0.96; 1.51)*	0.80 (0.66; 1.00)*	80

$F_f/F_{f\text{-}D}$ and $R_q/R_{q\text{-}D}$ are relative friction force and relative RMS roughness for friction force map correspondingly obtained with respect to median friction force and median RMS roughness of discocyte sample ($F_{f\text{-}D}$ = 621 arb. units, $R_{q\text{-}D}$ = 856 arb. units). Data are represented as Me (LQ; UQ).

* $p < 0.05$ in comparison with discocyte sample, Mann-Whitney *U* test.

Table 4
Young's modulus of erythrocyte surface.

Cell type	$E_f/E_{f\text{-}D}$, rel. units	n
Discocyte	1.00 (0.84;1.13)	52
Spherocyte	1.19 (1.01; 1.36)*	89

$E_f/E_{f\text{-}D}$ is relative elastic modulus obtained with respect to median elastic modulus of discocyte sample ($E_{f\text{-}D}$ = 65.8 MPa). Data are represented as Me (LQ; UQ).

* $p < 0.001$ in comparison with discocyte sample, Mann-Whitney *U* test.

in HS reflects the specific features of given pathology. Upon external tensile mechanical forces, normal erythrocytes can undergo a large mechanical deformation with further restoration to their original shape when the external force is no longer applied. When HS erythrocytes with the weakened linkage between the plasma membrane and actin-spectrin network experience large deformations, they are unable to recover their original shape after mechanical stress (Chang et. al., 2016). Using the quantitative flow cytometry method, Mullier found that HS blood contained higher levels of erythrocyte-derived microvesicles compared to healthy controls (Mullier et. al., 2012). Loss of the parts of membrane surface via vesiculation and the resulting cell shape change "discocytes-stomatocytes-spherocytes" are the characteristic morphological features of HS (Narla and Mohandas, 2017). Erythrocyte deformability is negatively correlated with vesiculation (Almizraq et al., 2013).

The results of our spectral analysis of the mechanical property maps for discocytes and spherocytes of HS patients agree with the mechanism of HS spherocyte formation via vesiculation. If the average distances between local contacts between the cytoskeleton and membrane in the surface layer of HS discocytes vary from 55 to 200 nm and can be grouped into three classes, the variation range of the corresponding distances for HS spherocytes is only about 75–145 nm with possible grouping into two classes. The structural network of membrane-cytoskeleton junctions in HS discocytes compared to that for HS spherocytes is less regular, with many large gaps. Under the mechanical stress conditions, the membrane area without the linkage to the cytoskeleton is removed with the consequent fusion of the membrane and condensation of the actin-spectrin network. The relatively high regularity and percentage of fine-mesh structure in HS spherocyte cytoskeleton leads to the increase in the parameters of both elastic properties and friction forces.

The increase of the content of stiff erythrocyte morphological forms (spherocytes) in HS blood causes the disturbance in blood flow (flow heterogeneity (Ye et al., 2018)) and oxidative stress in epithelial cells that can be also an additional mechanism of the change in the immunological profile and degree of cardiovascular risk in HS patients. These phenomena can play an important role in HS patients after splenectomy. The abnormal erythrocytes in HS patients with intact spleen are effectively removed from blood flow and changed for the young erythrocyte forms with higher deformability and lower stiffness. In post-splenectomy HS patients, the abnormal forms of erythrocytes with high stiffness and low deformability have a chance to remain in blood for a longer period. Thus, significant increases in platelets, leukocytes and monocytes were observed in splenectomised HS patients (Park et. al., 2017).

A limitation of the present study is the method of cell specimen preparation for AFM investigations that includes chemical fixation and partial drying of cells. The realized procedures are widely used in microscopy-based cytological studies. Both chemical fixation with glutaraldehyde and drying in the air change the state of cytoskeletal proteins and values of the parameters of the cell mechanical properties (the increase in glutaraldehyde concentration and drying time increases the stiffness of the cell surface layer (Hutter et. al, 2005)). However, the chemical fixation and drying make possible studying the architectonics and fine structure of mechanical property maps of the cell surface using AFM with the highest resolution in the air (Francis et. al., 2010). Additionally, fixation of cell surface structures allows effective application of the methods of the fractal and spatial-spectral analysis for revealing the parameters of the spatial distribution of mechanical properties on the cell surface. Because only one preparatory method was used for all the erythrocyte specimens one managed to conduct a comparative analysis of the structural and mechanical properties of HS discocytes and HS spherocytes.

5. Conclusion

The complex of the AFM parameters of the structural and mechanical properties of cell surface (the spectral and fractal parameters, the parameters of elastic and friction forces), so named as a physical-mechanical image of the cell surface layer (Starodubtseva et al., 2017a; Starodubtseva et al., 2017b), helps to understand the mechanical behavior of different morphological types of erythrocytes in blood stream of HS patients more in depth, as well as possible mechanisms of the development of HS complications. Our findings indicate that HS blood is highly heterogeneous in erythrocyte mechanical properties because of high percentage of spherocytes in HS blood and difference of the structural and mechanical properties of discoidal and spheroidal HS erythrocytes at the nano- and microscales. The morphological transformation of discocytes into spherocytes in HS leads to the change of elastic and frictional properties erythrocytes that can influence the immunological profile and the degree of cardiovascular risk in HS patients.

Conflict of interest

The authors do not have any conflict of interest in this study.

Acknowledgments

M.N.S gatefully acknowledges the support in form of the personal grant of the President of the Republic of Belarus in science. Authors thank Alexey Kondratchuk for technical support (cell sample preparation).

References

Alaarg, A., Schiffelers, R.M., van Solinge, W.W., van Wijk, R., 2013. Red blood cell vesiculation in hereditary hemolytic anemia. Front. Physiol. 4, 365.
Almizraq, R., Tchir, J.D., Holovati, J.L., Acker, J.P., 2013. Storage of red blood cells affects membrane composition, microvesiculation, and in vitro quality. Transfusion 53 (10), 2258–2267.
Chang, H.-Y., Li, X., Li, H., Karniadakis, G.E., 2016. MD/DPD multiscale framework for predicting morphology and stresses of red blood cells in health and disease. PLOS Comput. Biol. 12 (10), e1005173.
Deuticke, B., 2003. Membrane lipids and proteins as a basis of red cell shape and its alterations. In: Bernhardt, I., Ellory, J.C. (Eds.), Red Cell Membrane Transport in Health and Disease. Springer, Berlin, pp. 27–60.
Dulińska, I., Targosz, M., Strojny, W., Lekka, M., Czuba, P., Balwierz, W., Szymoński, M., 2006. Stiffness of normal and pathological erythrocytes studied by means of atomic force microscopy. J. Biochem. and Biophys. Meth. 66 (1–3), 1–11.
Eber, S., Lux, S.E., 2004. Hereditary spherocytosis - defects in proteins that connect the membrane skeleton to the lipid bilayer. Seminars Hematol. 41 (2), 118–141.
Francis, L.W., Gonzalez, D., Ryder, T., Baer, K., Rees, M., White, J.O., Conlan, R.S., Wright, C.J., 2010. Optimized sample preparation for high-resolution AFM characterization of fixed human cells. J. Micros. 240 (2), 111–121.
Ghosh, S., Chakraborty, I., Chakraborty, M., Mukhopadhyay, A., Mishra, R., Sarkar, D., 2016. Evaluating the morphology of erythrocyte population: an approach based on atomic force microscopy and flow cytometry. Biochim. et Biophys. Acta. 1858 (4), 671–681.
Girasole, M., Pompeo, G., Cricenti, A., Congiu-Castellano, A., Andreola, F., Serafino, A., Frazer, B.H., Boumis, G., Amiconi, G., 2007. Roughness of the plasma membrane as an independent morphological parameter to study RBCs: a quantitative atomic force microscopy investigation. Biochim. et Biophys. Acta 1768 (5), 1268–1276.
Hutter, J.L., Chen, J., Wan, W.K., Uniyal, S., Leabu, M., Chan, B.M., 2005. Atomic force microscopy investigation of the dependence of cellular elastic moduli on glutaraldehyde fixation. J. Micros. 219 (Pt 2), 61–68.
Kharin, Yu., 2013. Robustness in statistical forecasting. Springer, New-York, p. 356.
Kozlova, E.K., Chernysh, A.M., Moroz, V.V., Kuzovlev, A.N., 2013. Analysis of nanostructure of red blood cells membranes by space Fourier transform of AFM images. Micron 44, 218–227.
Li, X., Li, H., Chang, H.Y., Lykotrafitis, G. Em, Karniadakis, G., 2017. Computational biomechanics of human red blood cells in hematological disorders. J. Biomech. Eng. 139 (2), 021008.
Lim, H.W.G., Wortis, M., Mukhopadhyay, R., 2002. Stomatocyte-discocyte-echinocyte sequence of the human red blood cell: evidence for the bilayer-couple hypothesis from membrane mechanics. Proceedings National Academy Sci. United States America 99 (26), 16766–16769.

Liu, C., Derick, L.H., Palek, J., 1987. Visualization of the hexagonal lattice in the erythrocyte membrane skeleton. J. Cell Biol. 104, 527–536.
Lux 4th., S.E., 2016. Anatomy of the red cell membrane skeleton: unanswered questions. Blood 127 (2), 187–199.
Margetis, P., Antonelou, M., Karababa, F., Loutradi, A., Margaritis, L., Papassideri, I., 2007. Physiologically important secondary modifications of red cell membrane in hereditary spherocytosis - evidence for in vivo oxidation and lipid rafts protein variations. Blood Cells, Mol. Dis. 38 (3), 210–220.
Mullier, F., Bailly, N., Chatelain, C., Chatelain, B., Dogné, J., 2012. Quantification and characterization of microvesicles: applications in hereditary spherocytosis, type-II heparin-induced thrombocytopenia and cancer. Belgian J. Hematol. 3, 157–160.
Nans, A., Mohandas, N., Stokes, D.L., 2011. Native ultrastructure of the red cell cytoskeleton by cryo-electron tomography. Biophys. J. 101 (10), 2341–2350.
Narla, J., Mohandas, N., 2017. Red cell membrane disorders. International. J. Lab. Hematol. 39 (Suppl. 1), 47–52.
Park, J.B., Lee, S.A., Kim, Y.H., Lee, W.S., Hwang, J.J., 2017. Extramedullary hematopoiesis mimicking mediastinal tumor in a patient with hereditary spherocytosis: case report. Int. J. Surgery Case Rep. 41, 223–225.
Perrotta, S., Gallagher, P.G., Mohandas, N., 2008. Hereditary spherocytosis. Lancet 372 (9647), 1411–1426.
Smith, T.G., Lange, G.D., Marks, W.B., 1996. Fractal methods and results in cellular morphology — dimensions, lacunarity and multifractals. J. Neurosci. Methods 69 (2), 123–136.
Sokolov, I., Dokukin, M.E., 2017. Fractal analysis of cancer cell surface. Methods Mol. Biol. 1530, 229–245.
Starodubtseva, M., Chizhik, S., Yegorenkov, N., Nikitina, I., Drozd, E., 2010. Study of the mechanical properties of single cells as biocomposites by atomic force microscopy. In: Mendez-Vilas, A.O., Diaz, J. (Eds.), Microscopy: science. technology. applications and education. Formatex Research Center, Badajoz, pp. 470–477.
Starodubtseva, M.N., Starodubtsev, I.E., Starodubtsev, E.G., 2017a. Novel fractal characteristic of atomic force microscopy images. Micron 96, 96–102.
Starodubtseva, M.N., Starodubtsev, I.E., Yegorenkov, N.I., Kuzhel, N.S., Konstantinova, E.E., Chizhik, S.A., 2017b. Physical-mechanical image of the cell surface on the base of AFM data in contact mode. IOP Conference Series: Mater. Sci. Eng. 256, 012016.
Starodubtseva, M.N., Yegorenkov, N.I., Nikitina, I.A., 2012. Thermo-mechanical properties of the cell surface assessed by atomic force microscopy. Micron 43 (12), 1232–1238.
Ţălu, Ş., Stach, S., Kaczmarska, M., Fornal, M., Grodzicki, T., Pohorecki, W., Burda, K., 2016. Multifractal characterization of morphology of human red blood cells membrane skeleton. J. Micros. 262 (1), 59–72.
Xiong, Z., Oriss, T.B., Cavaretta, J.P., Rosengart, M.R., Lee, J.S., 2012. Red cell microparticle enumeration: validation of a flowcytometric approach. Vox Sanguinis 103, 42–48.
Ye, T., Shi, H., Phan-Thien, N., Lim, C.T., Li, Y., 2018. Relationship between transit time and mechanical properties of a cell through a stenosed microchannel. Soft Matter 14, 533–545.